Molecular dynamics simulations of aqueous NaCl solutions at high pressures and temperatures

John P. Brodholt [*]

Dept. of Geological Sciences, University College London, Gower Street, London, WC1E 6BT, UK

Abstract

Molecular dynamics simulations have been performed on aqueous NaCl solutions over a range of concentrations, pressures and temperatures. At 300 K and 1 bar, simulated solution densities are in very good agreement with the experimental data at concentrations from 0.2 m to 5.2 m. Simulated densities at 1 and 5 kbars with a 1.74 m concentration solution are also in very good agreement with the experimental data. At 300 K and 1 bar the solution is a true strong electrolyte with Na^+ and Cl^- ions being completely separated. As temperature increases NaCl pairs tend to form as a direct response to the decreasing dielectric constant. At very low values of the dielectric constant, higher order NaCl complexes are formed. Two simulations at 1 kbar and at temperatures in the two phase region show evidence for phase separation as all the ions cluster together into a small volume of the simulation box. This phase separation vanishes when the pressure is increased to 5 kbars. © 1998 Elsevier Science B.V. All rights reserved.

Keywords: Molecular dynamics; Simulations; NaCl solutions; High pressures; High temperatures

1. Introduction

NaCl is the most common solute in aqueous fluids in a wide variety of geological setting and, as such, its thermodynamic properties are essential for modelling and interpreting many geological processes. In particular, we need to know the densities of the single phase fluid for all salt concentrations at all lower crustal pressure and temperature conditions, together with the densities and composition of the coexisting fluid and vapour in the two phase region. The thermodynamic properties of the salt-water system are well known below about 573 K and 1 kbar, both in the two phase and single phase regions, and Archer (1992) has summarised these data and used

them to parameterise an equation of state. Above these conditions, however, experimental data become more scarce. For the two phase region Bischoff (1991) has summarised the available PVT data and Anderko and Pitzer (1993) have included these, together with data up to 5 kbars and 1173 K from synthetic fluid inclusion experiments (Bodnar, 1985), to fit their equation of state. Recently there have been some high P and T synthetic fluid inclusion experiments on very high concentration ($> 40\%$) $NaCl$–H_2O fluids (Bodnar, 1994), including some which report the effect of CO_2 (Schmidt et al., 1995). Above 5 kbars there are no experimental data on $NaCl$–H_2O fluids.

Molecular dynamics simulations have been very successful in predicting the properties of pure water and aqueous solutions. Potentials such as TIP4P

---
[*] Tel.: +44-171-387-7050.

Table 1
Simulations parameters

Atom	σ (Å)	ϵ (kJ/mol)	q (e)
O	3.166	0.65	−0.8476
H	0.0	0.0	0.4238
Na^+	2.35	0.54431	1.0
Cl^-	4.40	0.4187	−1.0

(Jorgensen et al., 1983) and SPC/E (Berendsen et al., 1987) treat the water molecule as a simple rigid body with coulombic charges on the oxygen and hydrogens to describe the dipole moment. These potentials are not polarisable and therefore maintain the same dipole moment regardless of the environment. Despite this obvious simplification, they have been successfully applied to a very wide range of problems and systems including aqueous salt solutions, organic solutions, hydrated clays, surface adsorption studies, to name but a few (Smith and Dang, 1994; Jorgensen and Tiradorives, 1995; Chialvo et al., 1995, Balbuena et al., 1996; Lin and Wood, 1996; Skipper et al., 1996; DeSiqueira et al., 1997). More physically reasonable polarisable potentials have also been developed but, although some properties of water are improved on, dielectric constants are generally worse than for the non-polarisable potentials (Sprik and Klein, 1988; Ahlström et al., 1989; Wallqvist and Karlström, 1989; Niesar et al., 1990; Van Belle et al., 1992; Dang, 1992; Brodholt et al., 1995a,b; Chialvo and Cummings, 1996). This is important when modelling salt solutions since the degree of ion association depends on the dielectric constant of the solvent.

In geological applications molecular dynamics simulations have been used over a very wide range of pressure and temperature conditions (Madura et al., 1988; Belonosko and Saxena, 1991; Kalinichev, 1991; Brodholt and Wood, 1990, 1993). In fact, molecular dynamics simulations produce PVT properties of fluids that are more reliable than simply extrapolating empirical equations of state. Synthetic fluid inclusion experiments on water up to 25 kbars and 1873 K (Brodholt and Wood, 1994) were found to agree extremely well with an equation of state based on densities taken from molecular dynamics simulations (Brodholt and Wood, 1993). In addition to predicting thermodynamic properties, molecular

dynamics simulations can offer substantial insight into the bonding and structural environment at an atomic scale. This is particularly important for aqueous solutions where accurate equations of state depend on a knowledge of the ion complexing.

In this paper results are presented from MD simulations on $NaCl–H_2O$ fluids over a range of pressure, temperature and concentrations. The agreement with experimental data is extremely encouraging and suggests that MD simulations can be used to predict accurately the thermodynamic properties of salt solutions. The fact that this approach is so successful for $NaCl–H_2O$ also suggests that it could be applied to other salt solutions, such as $CaCl_2$ and KCl or metal chloride solutions, where there is little or no experimental data.

2. Method

The molecular dynamics techniques used here are standard techniques, most of which can be found in the excellent book of Allen and Tildesley (1987). Simulations were preformed using the molecular dy-

Table 2
Summary of simulation results

Run	m (mol/kg)	T (K)	P (kbars)	ρ (g/cm^3)	ρ_{exp} (g/cm^3)
0	0.0	300	0.001	0.995	0.997[a]
1	0.21	300	0.001	1.011	1.005[b]
2	0.43	300	0.001	1.015	1.014[b]
3	0.86	300	0.001	1.033	1.030[b]
4	1.74	300	0.001	1.066	1.062[b]
5	3.48	300	0.001	1.116	1.120[b]
6	5.22	300	0.001	1.155	1.171[b]
7	1.74	570	1.00	0.872	0.900[b] 0.899[c]
8	1.74	785	1.00	0.601	0.727[b] 0.620[c]
9[d]	1.74	1000	1.00	⋯	⋯
10[d]	1.74	1273	1.00	⋯	⋯
11	1.74	2573	1.00	0.088	
12	1.74	785	5.00	0.915	0.916[c]
13	1.74	1273	5.00	0.654	0.668[c]

[a]Taken from the NBS equation of state for water (Haar et al., 1984).
[b]Experimental densities from the equation of state of Archer (1992). Experimental density for Run 11 is an extrapolation.
[c]Experimental densities from the equation of state of Anderko and Pitzer (1993).
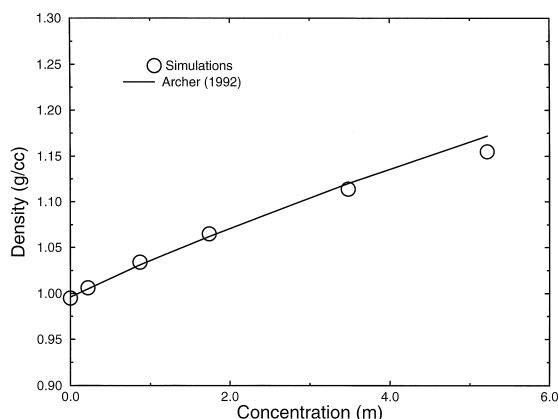[d]Runs 9 and 10 were in the two phase region.

Fig. 1. Simulation densities at 300 K and 1 bar at salt concentrations from 0.22 to 5.22 m. The straight line is from the equation of state of Archer (1992).

and

$$\epsilon_{ij} = \sqrt{\epsilon_i \epsilon_j} \,. \tag{3}$$

The parameters are given in Table 1. In all cases 256 water molecules were used and the number of NaCl pairs was varied from 1 to 24 depending on the concentration.

Dielectric constants of pure water were also calculated at the same pressure and temperature conditions as five simulations on the solutions in order to test its effect on ion pairing. These simulations were performed on a smaller system size of 108 molecules due to the much longer run times needed. Simulations of 200 ps were used in order to get reasonable statistics (Wasserman et al., 1995).

namics package DL_POLY 2.0. A modified Nose–Hoover constant NPT ensemble (Melchionna et al., 1993) was employed to control temperature and pressure, with a thermostat relaxation time of 0.5×10^{-12} s and a pressure (barostat) relaxation time of 0.8×10^{-12} s. The equations of motion were solved using a standard leapfrog scheme and a SHAKE algorithm for changing the cell volume. The rotational dynamics were treated using quarternions. A time step of 2 fs was used in all cases with total simulation times of 70 ps. These relatively long times were required to get reasonable statistics on the volume. The Ewald sum was used for all coulombic interactions.

The SPC/E intermolecular potential was used for water (Berendsen et al., 1987) and the ion–water interaction parameters were taken from Smith and Dang (1994). These parameters were determined by fitting to gas-phase binding enthalpy data for small sodium and chlorine ion–water clusters. The functional form for the interaction parameters are given as a Lennard–Jones potential

$$U_{ij} = 4\epsilon \left[\left(\frac{\sigma_{ij}}{r_{ij}} \right)^{12} - \left(\frac{\sigma_{ij}}{r_{ij}} \right)^6 \right] + \frac{q_i q_j}{r_{ij}} \tag{1}$$

where the normal mixing rules for ion–ion and ion–water cross terms apply

$$\sigma_{ij} = \frac{\sigma_i + \sigma_j}{2} \tag{2}$$

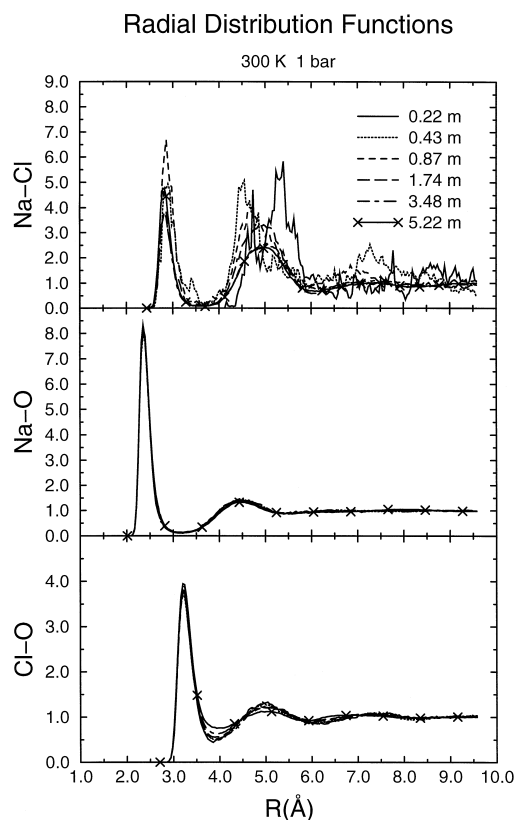## Radial Distribution Functions

Fig. 2. Radial distribution functions at 300 K and 1 bar at six concentrations from 0.22 m to 5.22 m. Essentially Na–O and Cl–O structure is independent of concentration under these conditions. The large amount of scatter in the Na–Cl radial distribution function is due to the fact that there is very little Na–Cl structure.

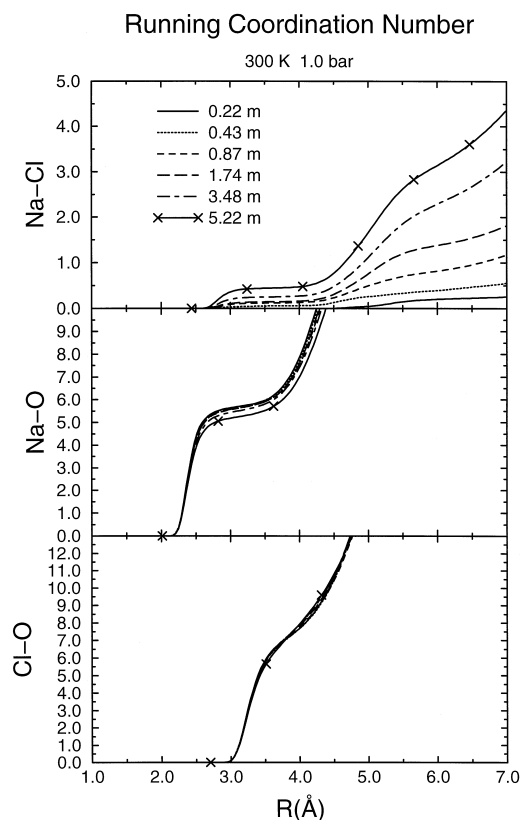## Running Coordination Number

300 K 1.0 bar

Fig. 3. Running coordination numbers, $n(r)$, for 300 K and 1 bar simulations. At low concentrations (0.22 m) there are no Na–Cl pairs closer than 4.0. As concentration increases there is some slight paring, but $n(r)$ remains below 0.5 even at saturation concentrations.

The statistical error on the simulated volumes are less than 1%. This was estimated by dividing a simulation of 70 ps into seven sets of 10 ps each and using the standard deviation of the seven different volumes as the uncertainty. A similar procedure gives an uncertainty in the pressure of 2%.

3. Results

3.1. Densities

A summary of the simulated densities at various concentrations and $P-T$ conditions is given in Table 2. For comparison, experimental densities as given by two equations of state are also included (Archer,

1992; Anderko and Pitzer, 1993). The equation of state of Archer (1992) accurately reproduces experimental data to 1 kbar, while that of Anderko and Pitzer (1993) is considered to be accurate from 573 K and saturation pressure to 5 kbars and 1200 K, which is the pressure and temperature limit of the experimental data.

At 1.0 bar and 300 K the densities from the simulations agree very well with the data from dilute to saturation concentrations (Fig. 1). At the highest concentration (5.22 m) the simulations begin to predict densities slightly lower than the data, although the difference is still less than 2%.

At higher pressures simulations were performed only at one representative concentration of 1.74 m. These densities are also in very good agreement with the data (Table 2). Two simulations at 1 kbar (9 and 10) are in the two-phase (liquid + vapour) region,
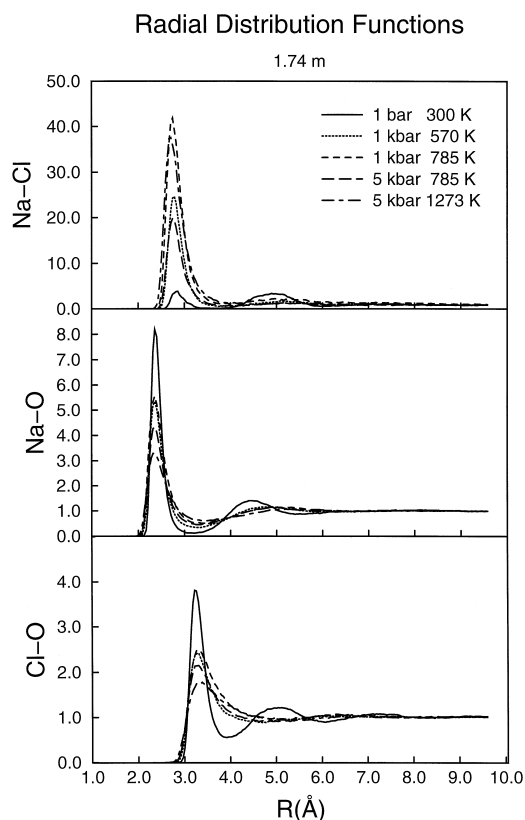
Radial Distribution Functions

1.74 m

Fig. 4. Radial distribution functions at 1.74 m and temperatures from 300 K to 1273 K and pressures of 0, 1 and 5 kbars.

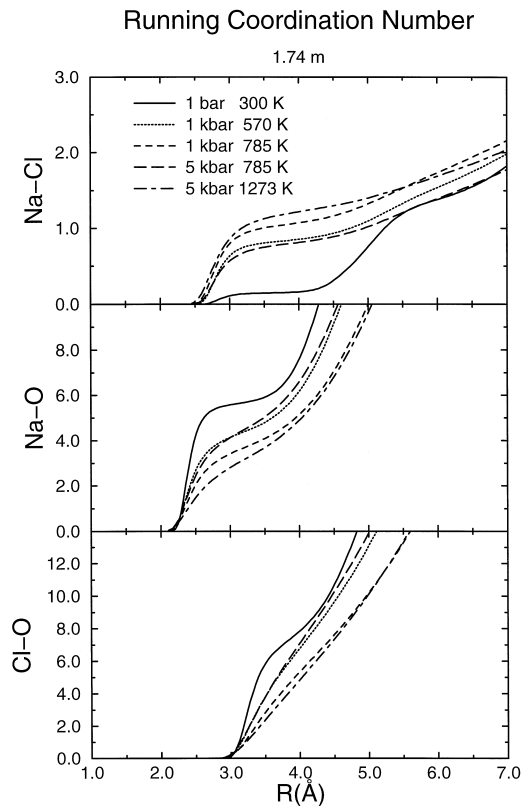## Running Coordination Number

1.74 m

Fig. 5. Running coordination numbers at a concentration of 1.74 m and temperatures from 300 K to 1273 K and pressures of 0, 1 and 5 kbars. Na–Cl coordination numbers increase substantially from room conditions which reflects the increasing dielectric constant of water.
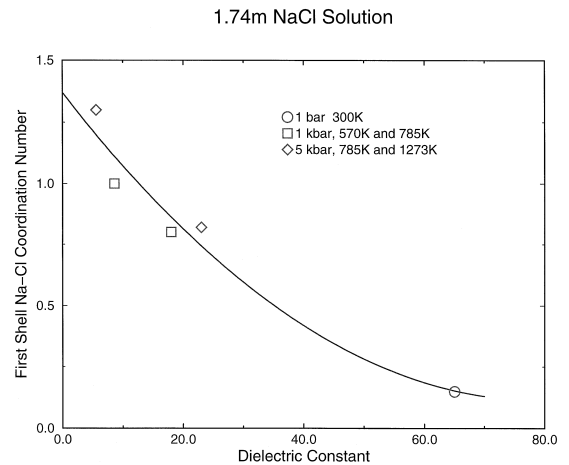
1.74m NaCl Solution

Fig. 6. First shell running coordination number at 1.74 m versus the dielectric constant of pure SPC/E water under the same pressure and temperature.

highlight the dangers in extrapolating with them. Simulations at 5 kbars also agree very well with the data.

3.2. Fluid structure

Fig. 2 shows the radial distribution functions, $g(R)$, at 1 bar and 300 K at concentrations from

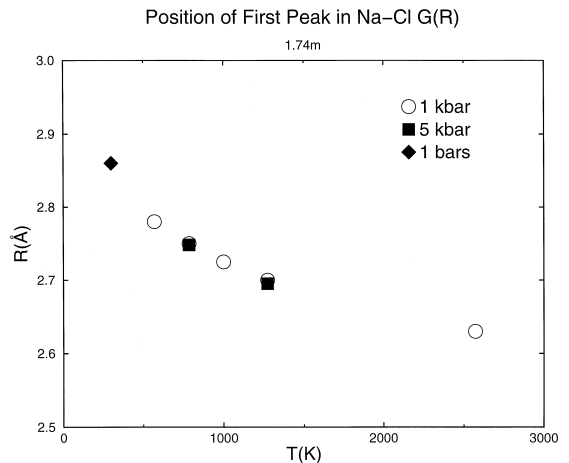### Position of First Peak in Na–Cl G(R)

1.74m

Fig. 7. Position of the first peak in $G(R)$ at a concentration of 1.74 m. Note that the peak position decreases strongly with temperature, but is relatively independent on pressure.

and since they show evidence of phase separation (discussed below), no densities are reported for them. The 1 kbar simulations are compared to both equations of state. At 570 K both equations of state predict the same density which is in excellent agreement with the simulation result. At 785 K, however, the equation of state of Archer (1992) overpredicts the density by about 15% relative to Anderko and Pitzer (1993) and the simulations. This is reasonable since Archer (1992) did not use any data at this temperature and pressure to fit to and did not claim that it is accurate under these conditions. It is instructive, however, in showing that equations of state which include many fit parameters break down quite severely when used even a little way outside the range of data that they are fit to, and serves to

0.22 m to 5.22 m, and Fig. 3 gives the running coordination number, $n(R)$, for the same simulations. Na–O and Cl–O radial distribution functions are essentially unaffected by concentration. The first coordination shell around the Cl^- ion contains 7.5 oxygens and a Cl–O distance of 3.2. This agrees well with 7.0 ± 0.4 oxygens and a Cl–O distance of

3.1 ± 0.1 obtained from neutron diffraction data on $NiCl_2$ Powell et al. (1993). For Na, the simulations gives between 5 and 6 oxygens (slightly decreasing with concentration) in the first hydration shell and a Na–O distance of 2.36. This also agrees well with available experimental data which find hydration shells of 4 and 6 water molecules and Na–O dis-
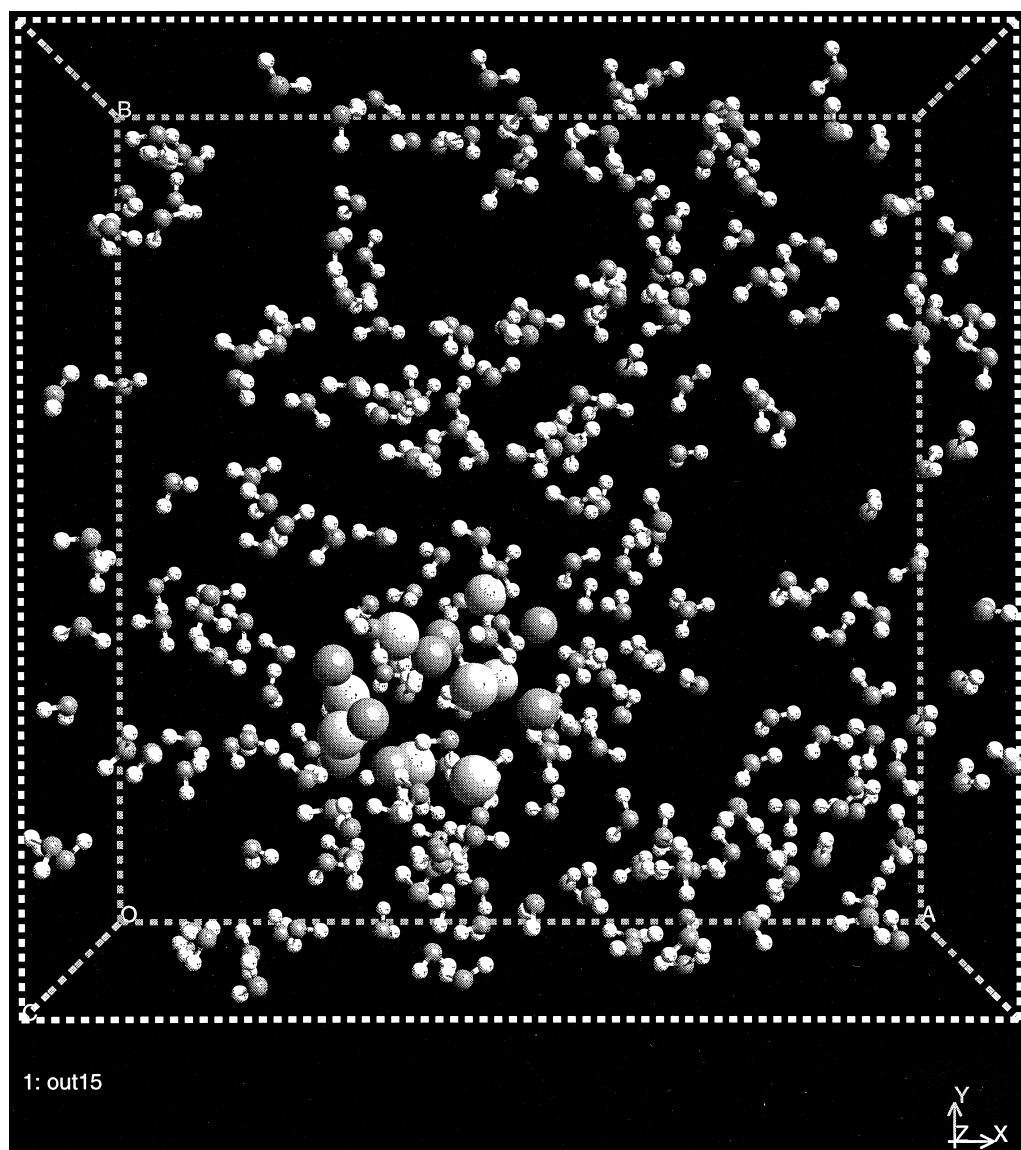

Fig. 8. Representative snapshot of one timestep in a simulation performed in the two-phase region. Note the strong clustering of Na^+ and Cl^- ions in one part of the simulation box (Na^+ ions are slightly bigger and lighter than the Cl^- ions). This clustering remains throughout the length of the simulation but is rapidly dispersed if the simulation pressure is increase to above the critical pressure.

tances of 2.38 and 2.4 in Na_2SO_4 and $NaBF_4$ solutions respectively (Neilson and Enderby, 1979).

The NaCl radial distribution functions are more variable with concentration and are much less smooth. This reflects the fact that there is very little systematic Na–Cl structure under these conditions (note that smooth $g(r)$s are obtained at higher temperatures when more NaCl pairing occurs (Fig. 4)). At the most dilute concentration (0.22 m) Na^+ and Cl^- ions never get within 4.0 of each other. There are some closer interactions at higher concentrations, but even at 5.22 m, the first shell coordination number is less than 0.5 (Fig. 3).

At higher pressures and temperatures the coordination environment for the Na^+ and Cl^- ions changes considerably. Figs. 4 and 5 show the radial distribution functions and running coordination numbers at 1.74 m concentration. Na–Cl pairing increases significantly with temperature and decreases with pressure. This is as expected since the dielectric constant of water strongly decreases with temperature and increases with pressure. This can be seen in Fig. 6 which shows the number of Na^+ ions in the Cl^- coordination shell (or vice versa) as a function of the dielectric constant of pure water calculated from simulations using the same intermolecular potential as in the mixtures (SPC/E). At 1273 K and 5 kbars the coordination number reaches 1.3 which implies the existence of triple ions and other higher order NaCl complexes, as suggested by Oelkers and Helgeson (1993a,b). In addition to ion clustering, the average Na–Cl distance decreases with temperature while being independent of pressure (Fig. 7).

The first hydration shell around the Na^+ and Cl^- ions is also substantially modified by temperature and pressure (Figs. 5 and 6). The number of water molecules around a Na^+ ion decreases strongly with temperature although the Na–O distance remains fixed at 2.36. Similarly, the number of water molecules in the first hydration shell around a Cl^- ion decreases with the O–Cl distance remaining roughly fixed between 3.2 and 3.3.

Under supercritical conditions and when the dielectric constant is less than 0.15, Oelkers and Helgeson (1993a,b) suggested the sequential formation of higher order complexes (pairs to triples, quadruples, etc.) as the salt concentration increases. Although this has not been tested directly here, the fact that higher order complexes do exist in low dielectric constant fluids is consistent with this idea and will be the focus of further study.

4. Immiscibility

Two simulations were performed within the two-phase region. This is reflected visually in the simulations since all the salt ions cluster very strongly in a small part of the simulation box. Fig. 8 is a representative snapshot from the simulation at 1273 K and 1 kbar. The obvious clustering of salt ions remains throughout the simulation (70 ps), but if the pressure is increased to 5 kbars the cluster rapidly splits up into NaCl ion pairs. This also occurs when the temperature is increase to 2500 K. The observation of phase separation in these simulations is interesting but it should be considered as preliminary since we have not tested systems size effects. This maybe an important consideration since the maximum size of the cluster is limited by the number of Na and Cl ions in the box. If true, however, it suggests a novel way of mapping out the two phase region.

5. Conclusions

Molecular dynamics simulations have been performed on NaCl aqueous solutions under ambient conditions on concentrations ranging from 0.22 m to 5.22 m, and at higher pressure and temperature conditions on a representative solution of 1.74 m. All simulated densities are in excellent accord with experimental data. Radial distribution functions and running coordination numbers describe basic features of the local hydration environment and ion pairing. Under ambient conditions Na^+ ions are surrounded by about 5.7 water molecules and Cl^- ions by about 7.5 water molecules. These both decrease strongly with temperature. The Na–Cl ion association increases from essentially no association at room conditions to clusters of more than one pair at 1273 K and 5 kbars. This is a direct function of the decreasing dielectric constant of the solvent. Finally, a surprising feature of the simulations is the separation of the NaCl ions from the bulk of the fluid when the P and T conditions are appropriate for the two phase region.

Acknowledgements

I am grateful to Dr. Vala Ragnarsdottir and Dr. Eric Oelkers for organising and inviting me to the Euroconference on the Geochemistry of Crustal Fluids. I thank the reviewers, and in particular Dr. Thomas Dreisner for his extremely thorough review. I am also grateful to the Royal Society for a University Research Fellowship.

References

Ahlström, P., Wallqvist, A., Angström, S., Jönsson, B., 1989. A molecular dynamics study of polarisable water. Molec. Phys. 14, 513–581.

Allen, M.P., Tildesley, D.J., Computer Simulation of Liquids. Clarendon Press, 1987.

Anderko, A., Pitzer, K.S., 1993. Equation-of-state representation of phase-equilibria and volumetric properties of the system NaCl–H_2O above 573 K. Geochim. Cosmochim. Acta 57, 1657–1680.

Archer, D.G., 1992. Thermodynamic properties of the NaCl + H_2O system: 2. Thermodynamic properties of NaCl(aq), NaCl·$2H_2O$(cr), and phase-equilibria. J. Phys. Chem. Ref. Data 21, 793–829.

Balbuena, P.B., Johnston, K.P., Rossky, P.J., 1996. Molecular-dynamics simulation of electrolyte-solutions in ambient and supercritical water: 1. Ion solvation. J. Phys. Chem. 100, 2706–2715.

Belonosko, A., Saxena, S.K., 1991. A molecular dynamics study of the pressure–volume–temperature properties of super-critical fluids: 1. H_2O. Geochim. Cosmochim. Acta 56, 381–387.

Berendsen, H.J.C., Grigera, J.R., Straatsma, T.P., 1987. The missing term in effective pair potentials. J. Phys. Chem. 91, 6269–6271.

Bischoff, J.L., 1991. Densities of liquids and vapors in boiling NaCl–H_2O solutions: a PVTX summary from 300 to 500°C. Am. J. Sci. 291, 309–338.

Bodnar, R.J., Pressure–volume–temperature-composition (PVTX) properties of the system NaCl–H_2O at elevated temperatures and pressures. PhD Thesis. Pennsylvania State University, 1985.

Bodnar, R.J., 1994. Synthetic fluid inclusions: XII. The system NaCl–H_2O. Experimental determination of the halite liquids and isochores for a 40 wt.% NaCl solution. Geochim. Cosmochim. Acta 58, 1053–1063.

Brodholt, J.P., Wood, B.J., 1990. Molecular dynamics of water at high pressures and temperatures. Geochim. Cosmochim. Acta 54, 2611–2616.

Brodholt, J.P., Wood, B.J., 1993. Simulations of the structure and thermodynamic properties of water at high pressures and temperatures. J. Geophys. Res. 98, 519–536.

Brodholt, J.P., Wood, B.J., 1994. Measurements of the PVT properties of water to 25 kbars and 1600°C from synthetic fluid inclusions in corundum. Geochim. Cosmochim. Acta 58, 2143–2148.

Brodholt, J.P., Sampoli, M., Vallauri, R., 1995a. Parameterizing polarizable intermolecular potentials for water with the ice 1 h phase. Molec. Phys. 85, 81–90.

Brodholt, J.P., Sampoli, M., Vallauri, R., 1995b. Parameterizing a polarizable intermolecular potentials for water. Molec. Phys. 86, 149–158.

Chialvo, A.A., Cummings, P.T., 1996. Engineering a simple polarisable model for the molecular simulation of water applicable over wide ranges of state conditions. J. Chem. Phys. 105, 8274–8281.

Chialvo, A.A., Cummings, P.T., Cochran, H.D., Simonson, J.M., Mesmer, R.E., 1995. Na^+–Cl^- ion pair association in supercritical water. J. Chem. Phys. 103, 9379–9387.

Dang, L.X., 1992. The nonadditive intermolecular potential for water revised. J. Chem. Phys. 97, 2659–2660.

DeSiqueira, A.V.C., Skipper, N.T., Coveney, P.V., Boek, E.S., 1997. Computer simulation evidence for enthalpy driven dehydration of smectite clays at elevated pressures and temperatures. Molec. Phys. 92, 1–6.

Haar, L., Gallagher, J.S., Kell, G.S., NBS/NRC Steam Tables. Hemisphere, Bristol, PA, 1984.

Jorgensen, W.L., Tiradorives, 1995. Free-energies of hydration for organic-molecules from Monte-Carlo simulations. Perspectives in Drug Discovery and Design 3, 123–128.

Jorgensen, W.A., Chandrasekhar, J., Madura, J.D., Impey, R.W., Klein, M.L., 1983. Comparison of simple functions for simulating water. J. Chem. Phys. 79, 926–935.

Kalinichev, A., 1991. Theoretical modeling of geochemical fluids under high-pressure, high-temperature conditions. High Pressure Research 7, 378–380.

Lin, C.L., Wood, R.H., 1996. Prediction of the free-energy of dilute aqueous methane, ethane, and propane at temperatures from 600 to 1200°C and densities from 0 to 1 g/cc using molecular-dynamics simulations. J. Phys. Chem. 100, 16399–16409.

Madura, J.D., Pettitt, B.M., Calef, D.F., 1988. Water under high pressure. Molec. Phys. 64, 325–336.

Melchionna, S., Ciccotti, G., Holiana, B.L., 1993. Hoover NPT dynamics for systems varying in shape and size. Molec. Phys. 78, 533–544.

Neilson, G.W., Enderby, J.E., 1979. Neutron and X-ray diffraction studies of concentrated aqueous electrolyte solutions. Annu. Rep. Prog. Chem., Sect. C 76, 185–220.

Niesar, U., Corongiu, G., Clementi, E., Kneller, G.R., Bhattacharya, D.K., 1990. Molecular dynamics simulations of liquid water using the ncc ab initio potential. J. Phys. Chem. 94, 7949–7956.

Oelkers, E.H., Helgeson, H.C., 1993a. Calculation of dissociation constants and the relative stability of polynuclear clusters of 1:1 electrolytes in hydrothermal solutions at supercritical pressures and temperatures. Geochim. Cosmochim. Acta 57, 2673–2697.

Oelkers, E.H., Helgeson, H.C., 1993b. Multiple ion association in supercritical aqueous solutions of single electrolytes. Science 261, 888–891.

Powell, D.H., Neilson, G.W., Enderby, J.E., 1993. The structure of Cl$^-$ in aqueous solution: an experimental determination of $g_{ClH}(r)$ and $g_{ClO}(r)$. J. Phys. Condens. Matter 5, 5723–5730.

Schmidt, C., Rosso, K.M., Bodnar, R.J., 1995. Synthetic fluid inclusions: X111. Experimental determination of PVT properties in the system $H_2O + 40$ wt.% NaCl + 5 mol% CO_2. Geochim. Cosmochim. Acta 59, 3953–3959.

Skipper, N.T., Bridgeman, C.H., Buckingham, A.D., Mancera, R.L., 1996. Computer simulation studies of the hydration and aggregation of simple hydrophobic molecules. Faraday Discussions 103, 141–150.

Smith, D.E., Dang, L.X., 1994. Computer simulations of NaCl association in polarizable water. J. Chem. Phys. 100, 3757–3766.

Sprik, M., Klein, M., 1988. A polarizable model for water using distributed charge sites. J. Chem. Phys. 89, 7556–7560.

Van Belle, D., Froeyen, M., Lippens, G., Wodak, S.J., 1992. Molecular dynamics simulation of polarizable water by and extended lagrangian method. Molec. Phys. 77, 239–255.

Wallqvist, A., Karlström, G., 1989. A new non-empirical force field for computer simulations. Chemica Scripta 29A, 131–137.

Wasserman, E., Wood, B., Brodholt, J., 1995. The static dielectric constant of water at pressure up to 20 kbars and temperatures to 1273 K: Experiment, simulations, and empirical equations. Geochim. Cosmochim. Acta 59, 1–6.